

Contents lists available at [ScienceDirect](https://www.sciencedirect.com)

## Journal of Biomechanics

journal homepage: [www.elsevier.com/locate/jbiomech](http://www.elsevier.com/locate/jbiomech)  
[www.JBiomech.com](http://www.JBiomech.com)

## Instrumentation of off-the-shelf ultrasound system for measurement of probe forces during freehand imaging

Tyler Schimmoeller<sup>a,b</sup>, Robb Colbrunn<sup>c</sup>, Tara Nagle<sup>c</sup>, Mark Lobosky<sup>d</sup>, Erica E. Neumann<sup>a,b</sup>, Tammy M. Owings<sup>a</sup>, Benjamin Landis<sup>a,b</sup>, J. Eric Jelovsek<sup>e</sup>, Ahmet Erdemir<sup>a,b,\*</sup><sup>a</sup> Department of Biomedical Engineering, Lerner Research Institute, Cleveland Clinic, Cleveland, OH, USA<sup>b</sup> Computational Bi modeling (CoBi) Core, Lerner Research Institute, Cleveland Clinic, Cleveland, OH, USA<sup>c</sup> BioRobotics and Mechanical Testing Core, Medical Device Solutions, Lerner Research Institute, Cleveland Clinic, Cleveland, OH, USA<sup>d</sup> Engineering Design Core, Medical Device Solutions, Lerner Research Institute, Cleveland Clinic, Cleveland, OH, USA<sup>e</sup> Department of Obstetrics and Gynecology, Duke University School of Medicine, Durham, NC, USA

## ARTICLE INFO

## Article history:

Accepted 21 November 2018

Available online xxxxx

## Keywords:

Ultrasound  
Load sensing  
Instrumentation  
Imaging

## ABSTRACT

Ultrasound is a popular and affordable imaging modality, but the nature of freehand ultrasound operation leads to unknown applied loads at non-quantifiable angles. The purpose of this paper was to demonstrate an instrumentation strategy for an ultrasound system to measure probe forces and orientation during freehand imaging to characterize the interaction between the probe and soft-tissue as well as enhance repeatability. The instrumentation included a 6-axis load cell, an inertial measurement unit, and an optional sensor for camera-based motion capture. A known method for compensation of the ultrasound probe weight was implemented, and a novel method for temporal synchronization was developed. While load and optical sensing was previously achieved, this paper presents a strategy for potential instrumentation on a variety of ultrasound machines. A key feature was the temporal synchronization, utilizing the electrocardiogram (EKG) feature built-in to the ultrasound. The system was used to perform anatomical imaging of tissue layers of musculoskeletal extremities and imaging during indentation on an in vivo subject and an in vitro specimen. The outcomes of the instrumentation strategy were demonstrated during minimal force and indentation imaging. In short, the system presented robust instrumentation of an existing ultrasound system to fully characterize the probe force, orientation, and optionally its movement during imaging while efficiently synchronizing all data. Researchers may use the instrumentation strategy on any EKG capable ultrasound systems if mechanical characterization of soft tissue or minimization of forces and deformations of tissue during anatomical imaging are desired.

© 2018 Published by Elsevier Ltd.

## 1. Introduction

Ultrasound is a non-invasive diagnostic tool commonly used for medical imaging and has seen increased use due to its many benefits over alternate imaging modalities (Bierig and Jones, 2009; Sippel et al., 2011). Most ultrasound imaging is performed freehand where the sonographer holds the probe in contact with the skin, adjusting the probe's orientation until the target region is located (Burcher et al., 2005; Mozaffari and Lee, 2017). Probe orientation has shown to be important for correct anatomical imaging, especially for ultrasound investigation of muscle impairments caused by multiple sclerosis and hemiparetic stroke

(Bénard et al., 2009; Carroll et al., 2005; Hafer-Macko et al., 2008). During anatomical imaging, the force exerted by the probe on the tissue is often minimized to view the tissue in a more anatomically correct, undeformed state (Chirita-Emandi et al., 2015; Yalcin et al., 2013). In a study of skin thickness at the bony prominences of spinal cord injury patients, the applied ultrasound probe force was minimized to maintain accurate, undeformed measurements (Yalcin et al., 2013). The probe force was also minimized to test the reliability of ultrasound based subcutaneous tissue thickness measurements (Chirita-Emandi et al., 2015). In ultrasound elastography, the applied load can influence the measured tissue deformations and may allow determination of elastic modulus. The compressive force must be minimized (or quantified) to determine the effective stiffness of the target region, e.g., a tumor, and its surrounding tissue (Nowicki and Dobruch-Sobczak, 2016). Minimal force application can be done by manually

\* Corresponding author at: Department of Biomedical Engineering (ND20), Lerner Research Institute, Cleveland Clinic, 9500 Euclid Avenue, OH 44195, USA.

E-mail address: [erdemira@ccf.org](mailto:erdemira@ccf.org) (A. Erdemir).

monitoring the force and adjusting accordingly (Burcher et al., 2005; Chirita-Emandi et al., 2015; Yalcin et al., 2013), and can be done automatically by using a force-controlled ultrasound system which maintains constant force by using a load cell and motor (Gilbertson and Anthony, 2012). During mechanical manipulation, e.g. indentation, quantifying the forces would allow characterization of the mechanics of the tissues (Behforootan et al., 2017a; Han et al., 2003; Pigula et al., 2016; Pigula-Tresansky et al., 2018; Zheng et al., 2000; Zheng and Mak, 1996). These use cases of ultrasound necessitate instrumentation of the ultrasound probes with force transducers, which has been done in several studies (Anthony, 2016; Burcher et al., 2005; Gilbertson, 2014; Gilbertson and Anthony, 2013, 2012; Han et al., 2003; Pigula et al., 2016; Pigula-Tresansky et al., 2018; Yohan Noh et al., 2015).

The two main challenges to measurements of loading during freehand ultrasound are related to compensation of probe weight due to gravity and temporal correlation of force data to ultrasound images. Weight compensation for the force of the ultrasound probe on the load cell was previously implemented using a secondary device to calibrate by measuring force at fixed known angles (Yohan Noh et al., 2015), however use of a secondary device may be cumbersome. Another method first establishes the gravitational directions with a plumb line, then the device is rotated around each axis about the center of mass while measuring the force and optically tracking the position (Burcher et al., 2005), however calibration is required prior to the collection of each image and requires additional equipment outside the scope of the instrumentation device itself. Weight compensation was also performed by using an accelerometer to measure the angle with respect to gravity and adjust the measured load accordingly (Gilbertson, 2014; Gilbertson and Anthony, 2013). An additional feature required to accompany weight compensation is ultrasound cable strain relief as established in past studies (Gilbertson, 2014; Gilbertson and Anthony, 2013). Temporal synchronization is required when data is collected from multiple sources. Methods to determine such time differences included the use of elaborate fixtures (Burcher et al., 2005) and a comparative analysis of image and position data after a sudden movement (Prager et al., 1999; Treece et al., 2003). In recent studies, EKG signal, which is visible on ultrasound images, was used for temporal synchronization (Behforootan et al., 2017b). However, it is not known whether an image analysis strategy or R-wave metadata extraction was utilized. An additional limitation in current devices is the lack of modularity, restricting use to a single ultrasound probe type (Burcher et al., 2005; Gilbertson, 2014; Gilbertson and Anthony, 2013, 2012; Han et al., 2003; Pigula et al., 2016; Yohan Noh et al., 2015).

The diversity of clinically available ultrasound systems and ultrasound probe sizes, where the selection is often dependent on the tissue of interest and depth of the target region, pose additional challenges to develop a universally applicable instrumentation strategy. Rapid probe removal was implemented previously, though it was limited to one probe type (Gilbertson, 2014; Gilbertson and Anthony, 2013; Yohan Noh et al., 2015). Additionally, the ability to equip a system with other sensors, e.g., motion capture, would increase its value from an extensibility perspective. Relating position and orientation of the probe to the subject would aid in three-dimensional reconstruction (Barber et al., 2009; Sun et al., 2013a, 2013b, 2014; Sun and Anthony, 2012; Treece et al., 2003; Yohan Noh et al., 2015).

The aim of this study was to develop and demonstrate the capabilities of comprehensive and extensible instrumentation system for measurement of probe loads during freehand imaging with a standard ultrasound system. Our ultimate goal was to realize a user friendly instrumented ultrasound system to further enable research and clinical use by eliminating several limitations of the existing instrumentation strategies. Specifically, the study focused

on the design and development of the following features that are critical for characterization of probe loading during ultrasound imaging: (1) automatic association and temporal synchronization of data collected from separate systems – ultrasound machine, and force measurement computer, (2) an integrated gravity compensation scheme, (3) easily interchangeable probes, and (4) extensibility to include additional instrumentation.

## 2. Method

### 2.1. System overview

A standard ultrasound system, ACUSON S3000™ (Siemens Healthcare, Erlangen, Germany), was integrated with a force measurement system. Integration included two different ultrasound probes (9L4 and 14L5) (Siemens), a 6-axis Nano25 load cell (ATI Industrial Automation, Apex, NC), and a VN-100 inertial measurement unit (IMU) (VectorNav, Dallas, TX). The load cell (SI-250-6 calibration) was connected to a data acquisition system (DAQ) (USB-6289, National Instruments, Dallas, TX). The IMU was equipped with a 3-axis gyroscope, 3-axis accelerometer, 3-axis magnetometer, and a barometric pressure sensor with an orientation alignment error of  $\pm 0.05$  degrees. A separate data acquisition system and data collection computer were utilized for measurements of force/torque and orientation data, which were sampled at 1000 Hz. Images were collected at 35 Hz on the ACUSON S3000™ ultrasound machine, the maximum sampling rate for this particular system.

An overview of the system is shown in Fig. 1. A connector block was used to send an analog signal from the external force/torque/orientation measurement computer to the ultrasound machine using the DAQ described above. This analog signal served the purpose of a post-processing based association of image and load measurement files and for temporal synchronization between image and load measurement systems. The DAQ interfaced both the connector block and force/torque/orientation controller to the computer, operating custom LabVIEW software (National Instruments, Dallas, TX).

### 2.2. Physical assembly

A casing was needed to integrate the load cell, IMU, and ultrasound probes as well as to mechanically isolate the probe from the sonographer to measure the probe's contact forces on the tissue. Each ultrasound probe was outfitted with a three-dimensional (3D) printed, removable sleeve to interface with the casing. The ultrasound probe assembly, consisting of the probe and sleeve, slid into the casing, where it was bolted to a stainless steel plate (Fig. 2). The steel plate was mounted to the load cell inside the casing where it received the ultrasound probe assembly.

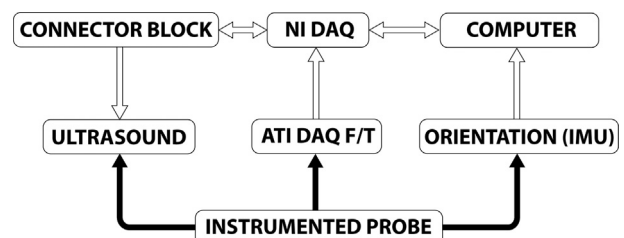


**Fig. 1.** The F/T controller refers to the force/torque load cell controller. The connector block is connected to the ultrasound via a quarter inch auxiliary jack. The DAQ and IMU connect to the computer via USB. The bold lines represent components of the handheld portion of the device.

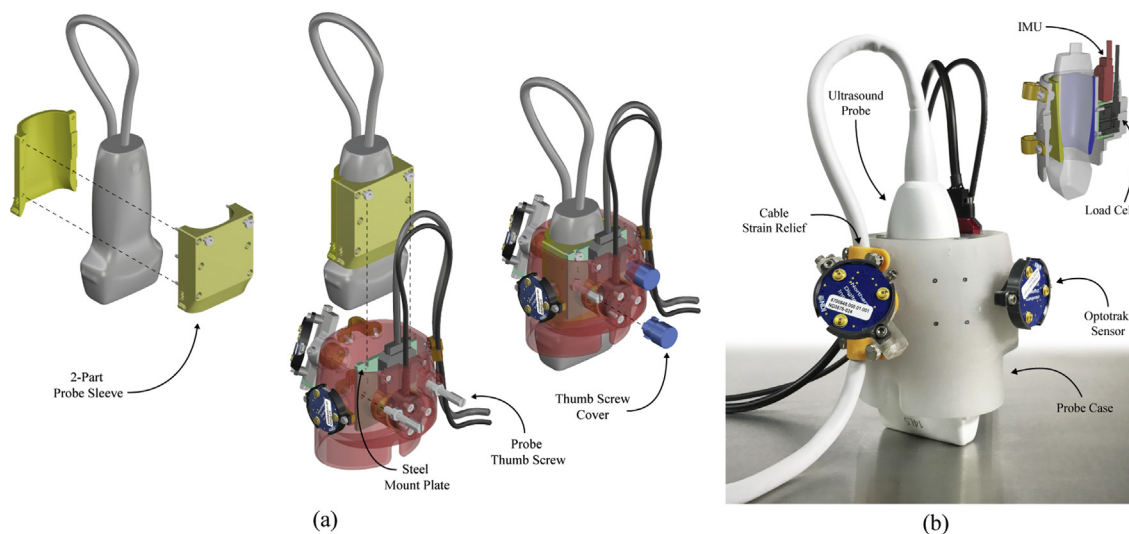


**Fig. 2.** (a) A computer-aided design model of the 9L4 ultrasound probe being encased by the 3D printed probe adapter (from left to right). Next, it slides in to the probe case and is secured with a set of thumb screws. The screw covers prevent interference with the load measuring portion of the apparatus by shielding them from the sonographer's hand. (b) A photograph of the actual device, with a CAD sectional drawing showing how load measuring portion is isolated from the outer handle.

Cable strain relief methods were used to offload the weight of cables, reducing their effect on the measured load in varying orientations. This was accomplished by fixing the ultrasound cable to the handle via custom 3D printed brackets. Similar brackets were used to secure the IMU and load cell.

### 2.3. Data collection software

A custom LabVIEW program was built upon simVITRO<sup>®</sup> LabVIEW packages (Cleveland Clinic, Cleveland, Ohio). The program was used to record all force/torque/orientation data, provide real time feedback on the resultant force, perform gravity compensation for the weight of the probe, generate and send an encoded analog signal to the ultrasound, and record all relevant subject metadata. An analog encoded signal was generated and sent to force/torque/orientation files and to the electrocardiogram (EKG) analog input of the ultrasound for the purpose of temporal synchronization and file association as a post-processing step. Additionally, the system recorded specifics of the subject including demographics, body height and mass, activity level, and anthropometric measurements. All subject information was stored in a subject XML, device configuration was saved in text files and all force/torque/orientation data were saved in an NI TDMS file (The NI TDMS File Format, 2018). The system was also designed to incorporate motion capture.

To compensate for the weight of the ultrasound probe, a gravity compensation process was performed to measure the mass and center of mass of the probe in the load cell reference frame. This step needs to be done only when the probe is changed. The 6-axis load cell and IMU were assumed to be rigidly attached to the ultrasound probe (Fig. 2). The spatial relationships of the orientation sensor, load cell and probe tip were previously measured using CAD models and implemented in the data measurement system as a selectable device configuration. After device assembly, the probe was manually positioned in six different orientations such that one of the load cell's major axes was oriented approximately along the direction of gravity, i.e., the positive x-axis of the load cell pointed up. At each of the six positions (Fig. 3), the orientation of the load cell and the load cell output were recorded. The readings collected from the six probe orientations and the spatial relationship between the load cell and the ultrasound probe tip were fed

into the built in LabVIEW function, Constrained Nonlinear Optimization, with unconstrained bounds, where the ultrasound probe mass, center of mass and the load cell offsets were optimized. The objective function calculated the 6-axis applied loads at the ultrasound tip for each orientation, summed the squared forces and squared torques for each orientation (weighting squared torques by 10) and summed the final values of the six orientations. The objective function was minimized such that the relationship between the probe orientation and probe weight was established to remove, or offset, the weight of the probe at any orientation.

### 2.4. Post processing

Temporal synchronization between force/torque/orientation data and ultrasound files was necessary because each was collected on an independent system. The EKG functionality built in to the ultrasound was used for this purpose. The ultrasound system analyzed the EKG to calculate heart-rate by finding the distance between each QRS complex (heart beat wave form), specifically the R-wave, which has the largest amplitude. The R-waves were stored in the DICOM (Digital Imaging and Communications in Medicine) metadata as an R Wave Time Vector, as per the international standard of medical imaging files formats (Digital Imaging and Communications in Medicine (DICOM) Standard, 2018). The analog signal generated by the system was designed to exhibit characteristics of a typical R-wave, specifically its amplitude and frequency, while encoding a binary message whereby an R-wave represented a 1, and lack thereof represented a 0. A unique sequence of R-waves were sent for each trial representing a 10-bit trial number followed by an 8-bit subject ID (Fig. 4). The time vector array calculated by the ultrasound was matched to the time vector array generated by the software, much like matching two patterns. As part of the matching process, the average temporal distance between all corresponding R-waves (i.e.  $R\text{-wave}_1_{US}$  and  $R\text{-wave}_1_{FT}$ ) was calculated and used as the value for temporal synchronization. This value was used to temporally align the force/torque/orientation data to its corresponding ultrasound frame, so that the appropriate data were reported for each image collected. All file association and temporal synchronization was performed using a custom Python ("Python," 2018) script. After matching,



Fig. 3. Measurements were taken in six different orientations to compensate for the weight of the ultrasound probe.

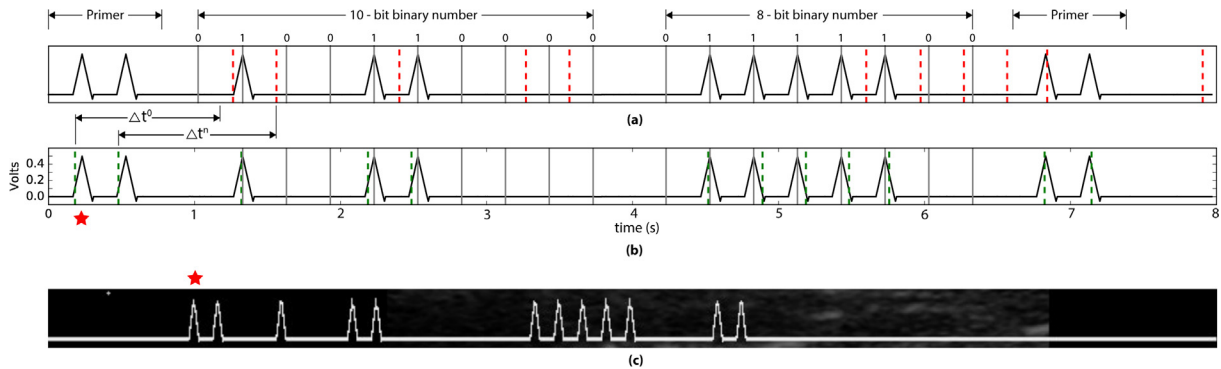


Fig. 4. The R-wave sequence is encoded as a binary message where a pulse denotes a 1 and lack of pulse a 0. (a) The simulated EKG as the triangle waves and the dashed lines as the unsynchronized R-waves extracted from the ultrasound metadata. (b) The temporal shift and alignment of the two signals. (c) A cropped portion of the ultrasound image where the EKG is plotted. The stars highlight the first wave.

the associated ultrasound files were partially renamed to include their appropriate trial number and subject identification number.

### 2.5. Validation of gravity compensation

Two experiments were performed to demonstrate the accuracy of probe weight offset and load transformation to probe tip during freehand use. At the beginning of each experiment the gravity compensation method was performed to account for the weight of the mock probe. The purpose of the first experiment was to demonstrate the probe weight offset in different orientations. The resultant force at the 14L5 ultrasound probe tip was measured in ten arbitrary orientations. The purpose of the second experiment was to demonstrate probe tip transformation (Fig. 5) by applying a known load to the tip at multiple orientations. A known weight of 4.82 N was suspended with a string from a 3D printed mock ultra-

sound probe after gravity compensation (Fig. 6). Again, the resultant force in ten arbitrary orientations was measured.

### 2.6. Minimal force imaging

Both the 14L5 and 9L4 ultrasound probes were used in conjunction with the instrumentation system. The 14L5 probe had a frequency bandwidth of 5–14 MHz (linear) and an imaging depth of 2–6 cm. The 9L4 probe had a frequency bandwidth of 4–9 MHz (linear) and an imaging depth of 5–6 cm. Gravity compensation was performed at the beginning of the session and after the probe type change. The 14L5 probe was used for the arm due to its optimization at lower depth and similarly the 9L4 was used primarily on the leg.

Minimal force imaging (<1 N) was performed on a 24 year old Asian male (BMI 24) at the anterior central upper arm with the 14L5 probe and at the anterior central upper leg with the 9L4

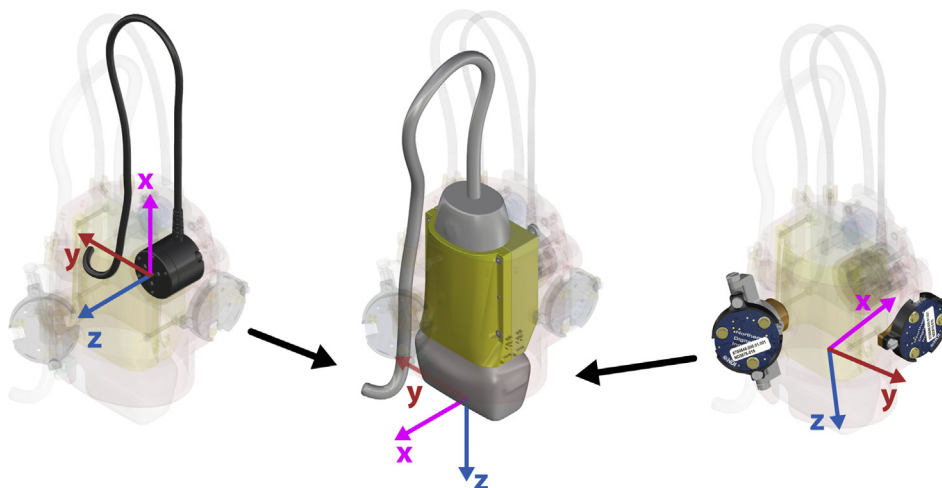


Fig. 5. The load cell origin was transformed to the probe tip to measure contact force and the motion capture origin was transformed to the probe tip to track aligned motion.



**Fig. 6.** A weight was suspended from the ultrasound mock probe tip after gravity compensation was performed. Measurements were taken in ten arbitrary orientations.

probe. The ultrasound probe was positioned so that its long axis aligned longitudinally with each appendage. At each location, a bone boundary was first located by the ultrasound, and while keeping the bone boundary in the frame, the operator adjusted the probe to manually minimize its force. The analog temporal synchronization signal was sent to the ultrasound for each trial. Once satisfied with the image positioning, the operator initiated data collection of both the ultrasound machine and LabVIEW program. The study was approved by the Cleveland Clinic Institutional Review Board and the Human Research Protection Office of the U.S. Army.

### 2.7. Imaging during indentation

Indentation was performed on the same subject described above in the same locations. Again, the 14L5 probe was used for the arm, followed by the 9L4 probe for the leg. At each location, the bone boundary was first found. Then, the operator initiated data collection and performed indentation until the tissue was compressed to a level that was comfortable for the subject. The operator was instructed to load and unload at a steady, consistent rate for each location.

### 2.8. Additional instrumentation

In additional experimentation, motion capture sensors were added to the instrumentation system to relate the position of the ultrasound to a cadaver leg specimen. The specimen was the right leg of a 55 year old Caucasian male (BMI 24), acquired for a larger set of related experiments. A set of smart LED clusters with an Optotrak Certus (Northern Digital Inc., Waterloo, ON) were used. Additional steps were required to relate the instrumented ultrasound to the specimen. The sensor, mounted to the 3D printed probe handle, was spatially related to the instrumented handle by digitizing divot points at known locations designed into the

3D printed casing. This relationship was used in conjunction with the scanned ultrasound probe geometry to transform the recorded motion to the ultrasound probe tip (Fig. 5).

## 3. Results

An ultrasound instrumentation system with integrated hardware and software was established. Software features included data collection, temporal synchronization, and gravity compensation. The physical device facilitated rapid probe change, isolation of the measured force from the user, and extensibility to include additional instrumentation.

The probe change consisted of loosening two bolts and the cable strain relief, removing the current probe, sliding in the new probe, tightening the two bolts and cable strain relief clamp, and performing gravity compensation. Altogether, the probe change procedure took two minutes with an experienced operator. The gravity compensation alone, which included measurements in six orientations and computationally calculating the offset, took 30 s. The remaining 90 s was the time required to switch probes.

All files were temporally synchronized and associated. The standard deviation of temporal synchronization was  $\pm 19.59$  ms, which represented the error in matching each corresponding R-wave from the analog signal.

Gravity compensation was verified with two experiments. The resultant force after performance of gravity compensation was measured to be  $0.02 \pm 0.01$  N. Next, a 4.82 N weight was suspended from the probe tip and the measured resultant force was  $4.83 \pm 0.03$  N.

During minimal force imaging, the sonographer was able to keep the force to  $<1$  N (Fig. 7). Three events were highlighted for minimal force imaging (Fig. 7), representing the first R-wave, the minimum force, and last R-wave.

The system was also capable of characterizing freehand indentation forces with the probe. For this use case (Fig. 8), the maximum indentation force was 10.74 N resulting in a total tissue compression of 18%. Force was mostly in the probe's longitudinal direction, while off-axis loads were the result of freehand movement. Four events were highlighted (Fig. 8): initial R-wave, start of indentation, mid-point of indentation, and peak resultant force. This provided the relationship between tissue deformation and force.

Additional instrumentation, i.e. Optotrak motion capture sensors, was integrated to the probe to measure probe movements. During indentation on a cadaver specimen, the probe moved about 7 mm along the z-axis of the probe tip coordinate system, which corresponded well to the total tissue deformation (Fig. 9).

## 4. Discussion

The aim of this paper was to develop and demonstrate an instrumentation strategy to increase the capability of any ultrasound imaging system to include measurement of probe forces and orientation. The motivation was based on the desire to monitor orientation and tissue loading to minimize soft tissue deformation during anatomical imaging (Bénard et al., 2009) and to record tissue deformation as a function of probe forces as seen in indentation studies (Han et al., 2003; Pigula et al., 2016; Pigula-Tresansky et al., 2018; Zheng et al., 2000; Zheng and Mak, 1996). We anticipate that the capability to instrument off-the-shelf ultrasound systems will facilitate research use of ultrasound for investigation of tissue mechanics and morphology, e.g., for diabetic foot examination. Ulceration risk of the foot due to complications of diabetes may be predicted by measuring plantar soft tissue stiffness (Naemi et al., 2017). Further, research use of shear wave elastogra-

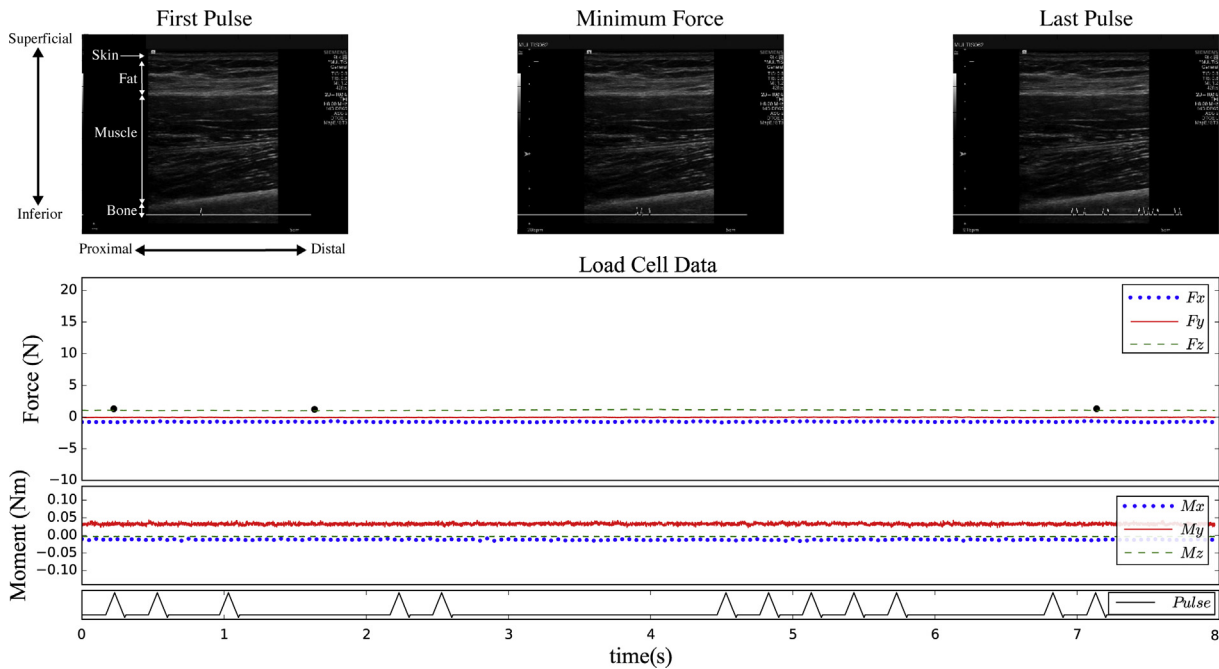


Fig. 7. Anatomical, minimal force imaging of an in vivo subject at the anterior central region of the upper leg. The three images are at the time of the first R-wave, minimum force, and last R-wave.

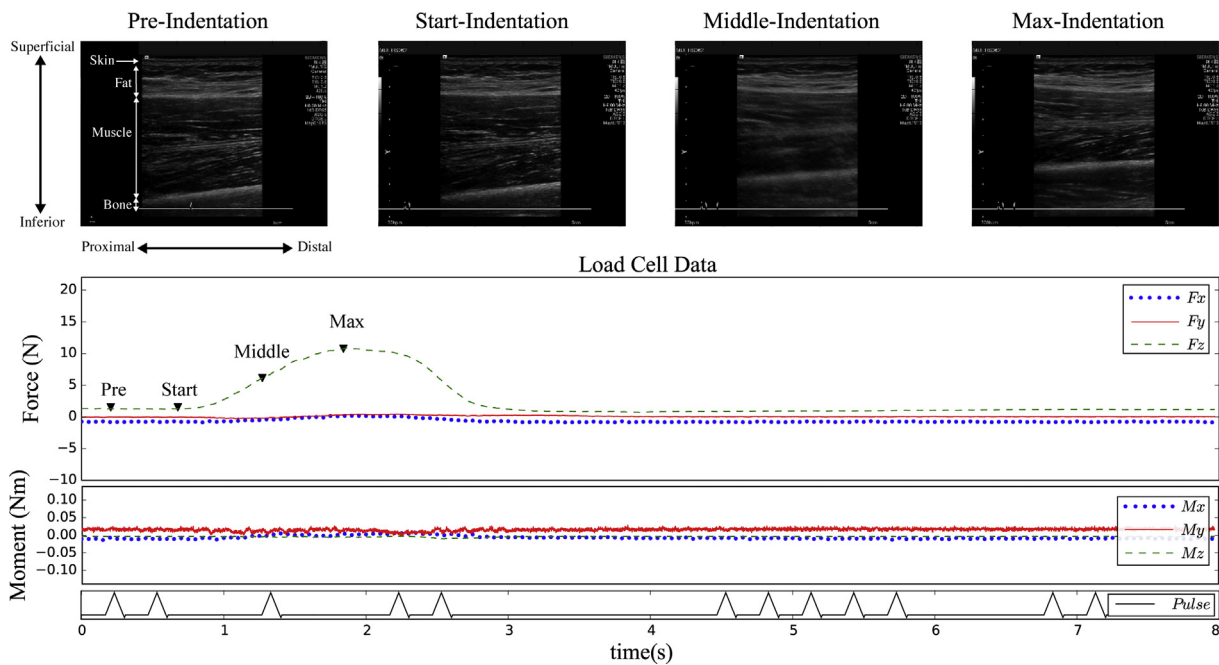
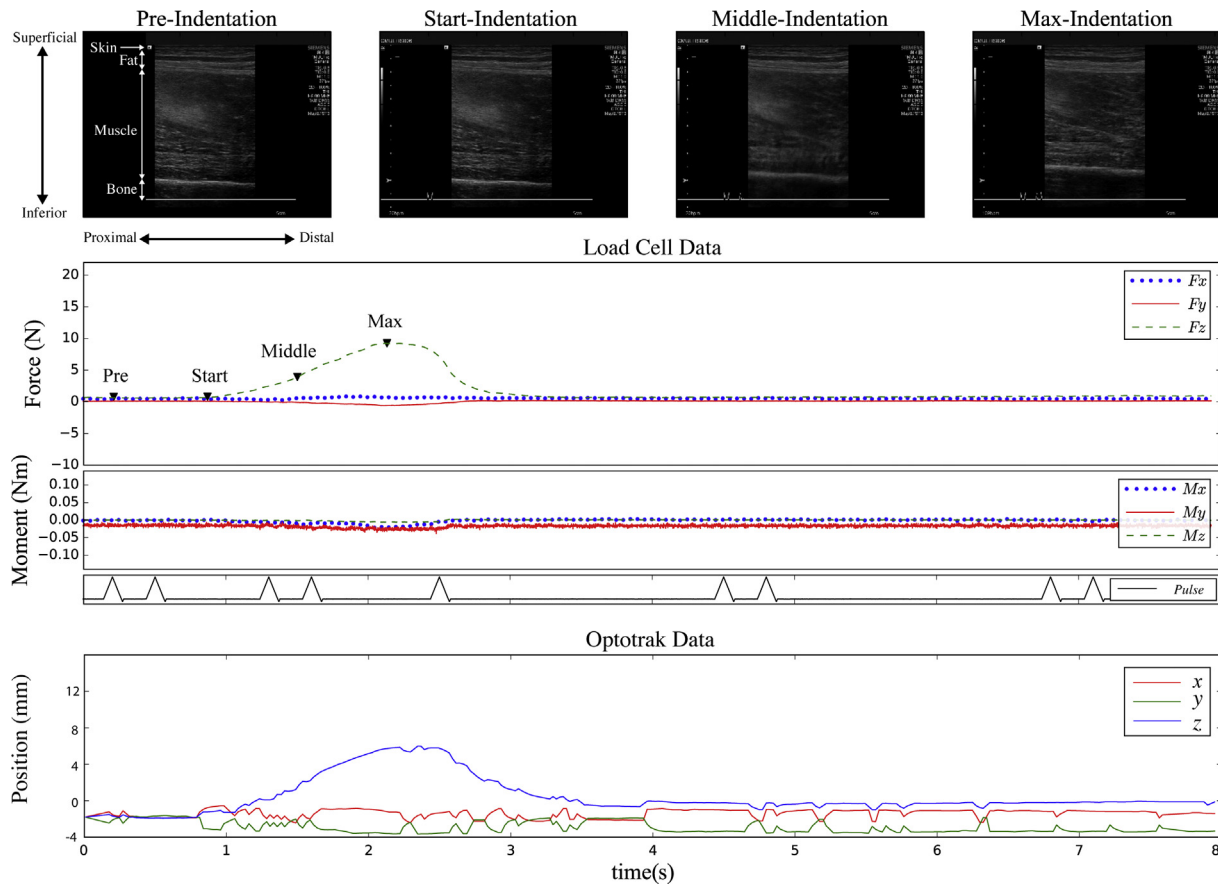


Fig. 8. Imaging during indentation of an in vivo subject at the anterior central region of the upper leg. The bone boundary moves up in the image as the probe indents the tissue. The temporal synchronization allowed correlation between applied force and ultrasound image at any given time point.

phy can be improved by measuring compression loads. It is known that finding the change in shear wave speed at varying magnitudes of applied load yields nonlinear tissue characterization (Chatzistergos et al., 2018).

In the current study, instrumentation was achieved by creating a method for efficient gravity compensation (30 s), a novel temporal synchronization, rapid interchangeable probe (~90 s), and extensibility to include other instrumentation. The system's efficiency and utility make it a useful diagnostic tool in a research setting.

The sonographer was also able to maintain minimal force (<1 N) during freehand operation. A small amount of shear loading was seen in each trial, likely due to the freehand nature of ultrasound operation and the heterogeneous structure of musculoskeletal tissue. The benefit of using a 6-axis load cell was that it fully characterized the mechanical interaction between the ultrasound probe and tissue. If a sonographer using this system applies a load in an unusual manner, it will be fully quantifiable, and if a repeatable measurement is desired, the 6-axis force characterization would quantify and validate the repeatability. The ability to reproduce



**Fig. 9.** Imaging during indentation of an in vitro specimen at the anterior central region of the upper leg. Camera based motion tracking was used to track the probe motion during indentation.

measurements proved valuable for analysis of musculoskeletal impairments (Bénard et al., 2009). Repeatability of applied load is also necessary in shear and strain elastography. The magnitude of the load may bias measured deformation characteristics of the tissue and its needs to be kept the same for comparisons of different populations (Behforootan et al., 2017b; Chatzistergos et al., 2018; Naemi et al., 2017).

In previous work, the force and position data were down sampled so that for every one position reading there was one force reading (Burcher et al., 2005). In the system presented here, the force/torque/orientation were collected on a single system making temporal synchronization innate and supporting maximum sampling rates. An expected error existed in temporally synchronizing the force/orientation data collected at 1000 Hz to the ultrasound image sequences sampled at 35 Hz as they are separate systems. This is a limitation of the ultrasound used in this study.

This system has already proved its usefulness in a separate study to measure multi-layer tissue thicknesses of musculoskeletal extremities for one hundred subjects (Neumann et al., 2018). The instrumentation facilitated the execution of this in vivo study, during which automatic file association and time synchronization was used for the 48 imaging locations on all subjects. Because the software was developed for this single use, expanding to use cases beyond the scope of the current project would require some modifications.

Several additional limitations to the methods exist. The cable strain relief requires the operator to limit contact with the cable loop so as not to affect the measured load. This limits the potential positions/orientations of the probe. The added weight, due to casing, may be ergonomically prohibitive for prolonged imaging, how-

ever, the operators for this study did not experience any fatigue. The system may be completely disassembled and sterilized with the exception to the load cell and IMU, which may be sterilized with sanitizing wipes as is currently done in standard ultrasound usage. Additionally, the ultrasound probes used in this device can be covered using standard transducer covers, as was done for this study. Overall, a robust instrumentation system was developed that can fully integrate with any existing ultrasound machine equipped with an EKG input. The system leverages additive manufacturing, making it compatible with many ultrasound probe types due to the system modularity. The following functionalities increase the accessibility and adaptability of instrumented ultrasound systems; capability to monitor loading for minimal force during anatomical imaging, quantifiable force during indentation, easy and quick operation for gravity compensation, automatic temporal synchronization and file association, the ability to rapidly change ultrasound probes, and extensibility to include additional instrumentation such as those of motion capture. All of the features previously mentioned enable research use by saving significant time in setup and in device operation. The design of the instrumentation, its specifications, post-processing source code, and sample data are currently available at the project site (<https://simtk.org/projects/multis>).

#### Acknowledgement

The authors would like to thank Siemens Medical Solutions USA, Inc. for loaning the ultrasound equipment. This study was part of the project titled "Reference Models for Multi-Layer Tissue Structures" which was conducted by the Cleveland Clinic and was made

possible by a contract vehicle which was awarded and administered by the U.S. Army Medical Research & Materiel Command under award number: W81XWH-15-1-0232. The views, opinions and/or findings contained in this document are those of the authors and do not necessarily reflect the views of the Department of Defense and should not be construed as an official DoD/Army position, policy or decision unless so designated by other documentation. No official endorsement should be made.

### Conflict of interest

The authors declare they have no conflict-of-interest in relation to this publication.

### Appendix A. Supplementary material

Supplementary data to this article can be found online at <https://doi.org/10.1016/j.jbiomech.2018.11.032>.

### References

- Anthony, B.W., 2016. Enhanced ultrasound for advanced diagnostics, ultrasound tomography for volume limb imaging and prosthetic fitting. In: Duric, N., Heyde, B. (Eds.), pp. 97900Q. <https://doi.org/10.1117/12.2214258>.
- Barber, L., Barrett, R., Lichtwark, G., 2009. Validation of a freehand 3D ultrasound system for morphological measures of the medial gastrocnemius muscle. *J. Biomech.* 42, 1313–1319. <https://doi.org/10.1016/j.jbiomech.2009.03.005>.
- Behforootan, S., Chatzistergos, P.E., Chockalingam, N., Naemi, R., 2017a. A simulation of the viscoelastic behaviour of heel pad during weight-bearing activities of daily living. *Ann. Biomed. Eng.* 45, 2750–2761. <https://doi.org/10.1007/s10439-017-1918-1>.
- Behforootan, S., Chatzistergos, P.E., Chockalingam, N., Naemi, R., 2017b. A clinically applicable non-invasive method to quantitatively assess the visco-hyperelastic properties of human heel pad, implications for assessing the risk of mechanical trauma. *J. Mech. Behav. Biomed. Mater.* 68, 287–295. <https://doi.org/10.1016/j.jmbm.2017.02.011>.
- Bénard, M.R., Becher, J.G., Harlaar, J., Huijting, P.A., Jaspers, R.T., 2009. Anatomical information is needed in ultrasound imaging of muscle to avoid potentially substantial errors in measurement of muscle geometry. *Muscle Nerve* 39, 652–665. <https://doi.org/10.1002/mus.21287>.
- Bierig, S.M., Jones, A., 2009. Accuracy and cost comparison of ultrasound versus alternative imaging modalities, including CT, MR, PET, and angiography. *J. Diagn. Med. Sonogr.* 25, 138–144. <https://doi.org/10.1177/8756479309336240>.
- Burcher, M.R., Noble, J.A., Man, L., Gooding, M., 2005. A system for simultaneously measuring contact force, ultrasound, and position information for use in force-based correction of freehand scanning. *IEEE Trans. Ultrason. Ferroelectr. Freq. Control* 52, 1330–1342. <https://doi.org/10.1109/TUFFC.2005.1509791>.
- Carroll, C.C., Gallagher, P.M., Seidle, M.E., Trappe, S.W., 2005. Skeletal muscle characteristics of people with multiple sclerosis. *Arch. Phys. Med. Rehabil.* 86, 224–229. <https://doi.org/10.1016/j.apmr.2004.03.035>.
- Chatzistergos, P.E., Behforootan, S., Allan, D., Naemi, R., Chockalingam, N., 2018. Shear wave elastography can assess the in-vivo nonlinear mechanical behavior of heel-pad. *J. Biomech.* 80, 144–150. <https://doi.org/10.1016/j.jbiomech.2018.09.003>.
- Chirita-Emandi, A., Dobrescu, A., Papa, M., Puiu, M., 2015. Reliability of measuring subcutaneous fat tissue thickness using ultrasound in non-athletic young adults. *Mædica* 10, 204–209.
- Digital Imaging and Communications in Medicine (DICOM) Standard, 2018. C.8.5.6, <[http://dicom.nema.org/MEDICAL/DICOM/2014c/output/chtml/part03/sect\\_C.8.5.6.html](http://dicom.nema.org/MEDICAL/DICOM/2014c/output/chtml/part03/sect_C.8.5.6.html)>.
- Gilbertson, M.W., 2014. Electromechanical Systems to Enhance the Usability and Diagnostic Capabilities of Ultrasound imaging (Thesis). Massachusetts Institute of Technology.
- Gilbertson, M.W., Anthony, B.W., 2013. An ergonomic, instrumented ultrasound probe for 6-axis force/torque measurement. In: Conf. Proc. Annu. Int. Conf. IEEE Eng. Med. Biol. Soc. IEEE Eng. Med. Biol. Soc. Annu. Conf. 2013, pp. 140–143.
- Gilbertson, M.W., Anthony, B.W., 2012. Ergonomic control strategies for a handheld force-controlled ultrasound probe. In: 2012 IEEE/RSJ International Conference on Intelligent Robots and Systems. Presented at the 2012 IEEE/RSJ International Conference on Intelligent Robots and Systems, pp. 1284–1291. <https://doi.org/10.1109/IRROS.2012.6385996>.
- Hafer-Macko, C.E., Ryan, A.S., Ivey, F.M., Macko, R.F., 2008. Skeletal muscle changes after hemiparetic stroke and potential beneficial effects of exercise intervention strategies. *J. Rehabil. Res. Dev.* 45, 261–272.
- Han, L., Noble, J.A., Burcher, M., 2003. A novel ultrasound indentation system for measuring biomechanical properties of in vivo soft tissue. *Ultrasound Med. Biol.* 29, 813–823.
- Mozaffari, M.H., Lee, W.-S., 2017. Freehand 3-D ultrasound imaging: a systematic review. *Ultrasound Med. Biol.* 43, 2099–2124. <https://doi.org/10.1016/j.ultrasmedbio.2017.06.009>.
- Naemi, R., Chatzistergos, P., Suresh, S., Sundar, L., Chockalingam, N., Ramachandran, A., 2017. Can plantar soft tissue mechanics enhance prognosis of diabetic foot ulcer? *Diabetes Res. Clin. Pract.* 126, 182–191. <https://doi.org/10.1016/j.diabres.2017.02.002>.
- Neumann, E., Owings, T., Schimmoeller, T., Nagle, T., Colbrunn, R., Landis, B., Jelovsek, J.E., Wong, M., Ku, J., Erdemir, A., 2018. Reference data on thickness and mechanics of tissue layers and anthropometry of musculoskeletal extremities. *Sci. Data* 5, 180193.
- Nowicki, A., Dobruch-Sobczak, K., 2016. Introduction to ultrasound elastography. *J. Ultrason.* 16, 113–124. <https://doi.org/10.15557/JoU.2016.0013>.
- Pigula, A.J., Wu, J.S., Gilbertson, M.W., Darras, B.T., Rutkove, S.B., Anthony, B.W., 2016. Force-controlled ultrasound to measure passive mechanical properties of muscle in Duchenne muscular dystrophy. In: Presented at the 2016 38th Annual International Conference of the IEEE Engineering in Medicine and Biology Society (EMBC), pp. 2865–2868.
- Pigula-Tresansky, A.J., Wu, J.S., Kapur, K., Darras, B.T., Rutkove, S.B., Anthony, B.W., 2018. Muscle compression improves reliability of ultrasound echo intensity. *Muscle Nerve* 57, 423–429. <https://doi.org/10.1002/mus.25779>.
- Prager, R.W., Gee, A., Berman, L., 1999. Stradx: real-time acquisition and visualization of freehand three-dimensional ultrasound. *Med. Image Anal.* 3, 129–140.
- Python [WWW Document], 2018. URL <https://www.python.org/> (accessed 9.21.17).
- Sippel, S., Muruganandan, K., Levine, A., Shah, S., 2011. Review article: use of ultrasound in the developing world. *Int. J. Emerg. Med.* 4, 72. <https://doi.org/10.1186/1865-1380-4-72>.
- Sun, S.Y., Anthony, B.W., 2012. Freehand 3D ultrasound volume imaging using a miniature-mobile 6-DOF camera tracking system. In: Presented at the 2012 9th IEEE International Symposium on Biomedical Imaging (ISBI), pp. 1084–1087.
- Sun, S.-Y., Gilbertson, M., Anthony, B.W., 2014. Probe localization for freehand 3D ultrasound by tracking skin features. In: Medical Image Computing and Computer-Assisted Intervention – MICCAI 2014, Lecture Notes in Computer Science. Presented at the International Conference on Medical Image Computing and Computer-Assisted Intervention. Springer, Cham, pp. 365–372.
- Sun, S.Y., Gilbertson, M., Anthony, B.W., 2013a. 6-DOF probe tracking via skin mapping for freehand 3D ultrasound. In: Presented at the 2013 IEEE 10th International Symposium on Biomedical Imaging, pp. 780–783.
- Sun, S.Y., Gilbertson, M., Anthony, B.W., 2013b. Computer-guided ultrasound probe realignment by optical tracking. In: Presented at the 2013 IEEE 10th International Symposium on Biomedical Imaging, pp. 21–24.
- The NI TDMS File Format [WWW Document], 2018. URL <http://www.ni.com/white-paper/3727/en/> (accessed 9.22.17).
- Treece, G.M., Gee, A.H., Prager, R.W., Cash, C.J.C., Berman, L.H., 2003. High-definition freehand 3-D ultrasound. *Ultrasound Med. Biol.* 29, 529–546. [https://doi.org/10.1016/S0301-5629\(02\)00735-4](https://doi.org/10.1016/S0301-5629(02)00735-4).
- Yalcin, E., Akyuz, M., Onder, B., Unalan, H., Degirmenci, I., 2013. Skin thickness on bony prominences measured by ultrasonography in patients with spinal cord injury. *J. Spinal Cord Med.* 36, 225–230. <https://doi.org/10.1179/2045772312Y.0000000088>.
- Noh, Yohan, Housden, R.J., Gomez, A., Knight, C., Garcia, F., Liu, Hongbin, Razavi, R., Rhode, K., Althoefer, K., 2015. An ergonomic handheld ultrasound probe providing contact forces and pose information. In: Conf. Proc. Annu. Int. Conf. IEEE Eng. Med. Biol. Soc. IEEE Eng. Med. Biol. Soc. Annu. Conf. 2015, pp. 5773–5776.
- Zheng, Y.-P., Choi, Y.K., Wong, K., Chan, S., Mak, A.F., 2000. Biomechanical assessment of plantar foot tissue in diabetic patients using an ultrasound indentation system. *Ultrasound Med. Biol.* 26, 451–456.
- Zheng, Y.-P., Mak, A.F.T., 1996. An ultrasound indentation system for biomechanical properties assessment of soft tissues in-vivo. *IEEE Trans. Biomed. Eng.* 43, 912–918. <https://doi.org/10.1109/10.532125>.